Response Surface Optimized Nanoemulgel for Ocular Bimatoprost Delivery: Integrating Hyaluronic Acid and Omega-3 to Enhance Residence Time and Alleviate Side Effects in Glaucoma

Monika Singh[a], Samrat Chauhan[b], Monika[a], Rahul Pratap Singh[a], Saahil Arora[a], Vikas Jhawat[a*]

[a]Department of Pharmaceutical Science, School of Healthcare and Allied Science, GD Goenka University, Gurugram, Haryana, India

[b]Department of Pharmacy, Chitkara University, Rajpura, Punjab, India

Corresponding Author:

Dr. Vikas Jhawat

Associate Professor, Department of Pharmaceutical Science, School of Healthcare and Allied Science, GD Goenka University, Gurugram, Haryana, India

Email: Jhawat231287@gmail.com

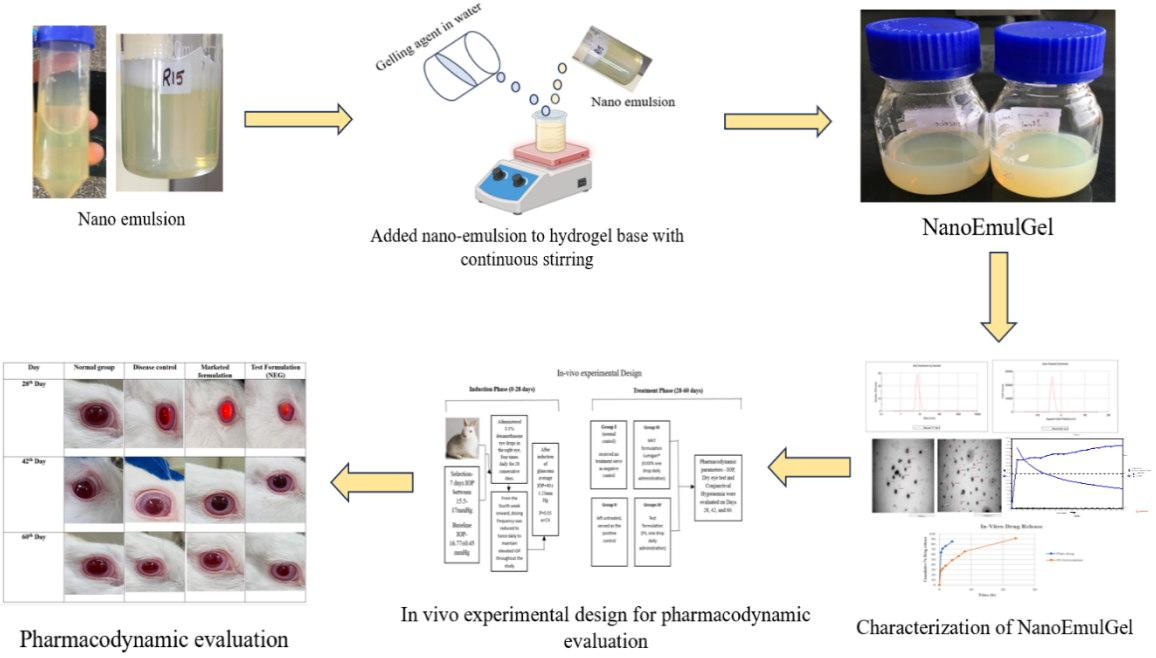

Graphical Abstract: Development of ocular nanogel for the mitigation of the adverse effects associated with anti-glaucoma medications

Abstract

Purpose: The objective of the present study was to conduct a pharmacological evaluation of a topical sustained release in-situ nanoemulgel (NEG) containing hyaluronic acid (HA) and omega-3 fatty acid in the mitigation of adverse drug reactions induced by antiglaucoma drugs.

Method: Bimatoprost, HA, algal oil (oil phase and source of omega-3 fatty acid), tween 80 (emulsifier I), Span 80 (emulsifier II), and water (aqueous phase) were used for the formulation development, and high-pressure homogenization followed by ultrasonication method was adopted to prepare nano-emulsion.

Result: Formulation optimization was done by using a response surface methodology (RSM) and evaluated for particle size, Zeta potential, polydispersity index (PDI). The optimized formulation was transformed into a gelling

system using gellan gum (GG). The prepared NEG was subsequently subjected to both in vitro and in vivo evaluations. The optimized nanoemulsion was composed of 0.03% bimatoprost, 7.5% oil, 22.5% tween 80 and span 80 [Smix (4:1)], 0.18% HA, and 70% water. It exhibited a particle size of 40.67 ± 0.74 nm, a zeta potential of 36.4 ± 0.98 mV, and a PDI of 0.246 ± 0.043. NEG was prepared with 0.250% of GG. When combined with simulated tear fluid, the formulated NEG converted from a sol to a gel, confirming it's in situ gelation capability. The optimized formulation exhibited a drug content of 98.76 ± 0.54%. *In vitro* release studies revealed a sustained drug release and was further confirmed to be stable, isotonic, and sterile. Pharmacodynamic evaluation demonstrated a significant reduction in intraocular pressure (IOP) with the developed NEG.

Conclusion: The developed formulation mitigates common adverse effects of anti-glaucoma therapy, including dry eye and conjunctival hyperemia, through the incorporation of HA and omega-3 fatty acid.

Keywords: Glaucoma, Anti-glaucoma medications, Adverse drug reactions, Bimatoprost, HA, Omega-3 fatty acid, NEG.

How to cite this article: Singh M, Chauhan S, Monika, Singh RP, Arora S, Jhawat V. Response Surface Optimized Nanoemulgel for Ocular Bimatoprost Delivery: Integrating Hyaluronic Acid and Omega-3 to Enhance Residence Time and Alleviate Side Effects in Glaucoma. Int J Drug Deliv Technol. 2026;16(6s): 900-909; DOI: 10.25258/ijddt.16.6s.119

Introduction

Glaucoma refers to an increase in intraocular pressure caused by improper drainage of fluid from the eye. This elevated pressure can injure the optic nerve over time, potentially leading to visual impairment (1). Glaucoma is the most serious eye disease and the second cause of blindness. Around 80 million people worldwide are affected by glaucoma, and this number is expected to increase to about 100 million by 2040 (2,3).

Prostaglandin analogues, Rho-kinase inhibitors, beta-blockers, carbonic anhydrase inhibitors, and alpha-2 adrenergic agonists have been the first-line therapy for glaucoma. Along with therapeutic effects, topical administration of antiglaucoma medications showed potential adverse effects associated with their long-term use. According to NDA labels, conjunctival hyperemia is the most frequent adverse reaction, reported in ~25–45% of Lumigan® (Bimatoprost) users and ~53% of Netarsudil (Rhopressa) users. Extensive evidence underscores the ocular adverse effects associated with antiglaucoma therapies. Prostaglandin analogues, the preferred first-line agents, often cause conjunctival hyperemia, iris pigmentation, eyelash changes, and periocular skin darkening (4), while beta-blockers may induce hyperemia, reduced corneal sensitivity, and epithelial keratopathy; Rho-kinase inhibitors are frequently associated with hyperemia (48–60%) along with cornea verticillate, limbal microhemorrhages, ocular discomfort, burning, blurred vision, transient visual decline, and excessive tearing (5). Küçük E. et al. (2024) reported that among patients receiving antiglaucoma therapy, 27% experienced dry eye. (6). Studies reported that long term use of topical anti-glaucoma medications damages the ocular surface by inducing inflammatory changes in the conjunctiva, reducing goblet cells, and altering epithelial and dendritic cell structure, leading to compromised conjunctival cytology and tear film stability (7-14). These drugs also disrupt Meibomian gland anatomy and physiology, decrease tear production and turnover, and cause corneal epithelial damage, collectively resulting in altered ocular surface morphology and function (9,15). Therefore, mitigation of these adverse reactions are crucial to enhance therapeutic efficacy and improving the overall management of glaucoma.

Components like Omega-3 fatty acid and HA can help to address ADRs associated with anti-glaucoma medications. Omega-3fatty acid is reported to be helpful in the restoration of ocular surface damage and morphological changes. Hyaluronic acid (HA) also supports the management of dry eye by suppressing inflammatory mediators and enhancing both tear film stability and tear secretion (16–19). It is a well-recognized agent in the treatment of dry eye and various ocular surface disorders. HA has been shown to alleviate conjunctivitis (20), minimize damage to the ocular surface (21, 22), ease dry eye symptoms (23), reduce inflammation (24), promote corneal healing, and aid in corneal stromal regeneration (25, 26).

Bimatoprost is an FDA-approved prostaglandin analogue commonly prescribed for glaucoma management. It lowers intraocular pressure by promoting aqueous humor drainage through both the uveoscleral route and the trabecular meshwork (27). Gellan gum (GG), an ion-

sensitive polymer, undergoes phase transitions under ocular physiological conditions and has therefore been employed in ocular drug delivery applications (28). The aim of the present work is to develop and evaluate an ocular drug delivery system designed to increase ocular residence time, enable sustained drug release, improve therapeutic outcomes, and make it patient friendly.

Materials and Methods

Materials

Bimatoprost for this study was procured from Shanghai Terns Tech Co. Ltd., based in Shanghai, China. The algal oil was provided by Empirical Aromatics, situated in the Surajpur Industrial Area of Greater Noida, Uttar Pradesh. Tween 80 and Span 80 were purchased from Upasana Enterprises in Gurgaon, Haryana, whereas gellan gum (GG) was sourced from Otto Chemie Pvt. Ltd. in Mumbai, Maharashtra. Every chemical and excipient applied in the experiments met analytical-grade standards.

Analysis of Bimatoprost

Reverse-phase high-performance liquid chromatography (RP-HPLC) was employed to evaluate bimatoprost on a Waters e2695 instrument. Separation was achieved with a SunFire C18 column measuring 250 mm in length, 4.6 mm in internal diameter, and featuring 5 µm particles. The procedure involved isocratic elution using a mobile phase composed of potassium dihydrogen phosphate buffer (adjusted to pH 2.8 ± 0.05) mixed with acetonitrile at a 55:45 ratio, delivered at 1 mL/min. Detection occurred via UV absorbance at 210 nm, with the full analysis completing in 6 minutes and the bimatoprost peak eluting at approximately 2.8 ± 0.1 minutes (29).

Preparation of bimatoprost containing nano emulsion

The method of preparation and formula used were selected based on the data obtained from trial formulations. The weighed amount of drug was dissolved in algal oil at 65-75°C on a magnetic stirrer with a heater at high stirring until it dissolved completely. Span 80 and tween 80 (1:4) were added with continuous stirring at 70°C temperature for 20 minutes. Prepared aqueous phase by dissolving HA in water and maintained the temperature at 70°C. After 20 min, the aqueous phase was added into the oily phase slowly with continuous stirring. Now, the prepared emulsion was homogenized at 12000 rpm for 30 minutes and ultrasonicated for 5 minutes to get a nano emulsion.

Optimization of nano emulsion with RSM

Design Expert Software (Version 12, Stat-Ease, Inc., MN, USA) was used to develop a Box–Behnken Design (BBD) consisting of 17 experimental formulations based on a 3^3 matrix. The selected independent factors were oil (X1), Smix (X2), and water (X3), while the measured responses included particle size (Y1), zeta potential (Y2), and PDI (Y3) (Table 1). The assigned levels of each independent variable used to generate the design trials are listed in Table 2. A polynomial model was applied to describe how the variables influenced the responses through linear, quadratic, and interaction effects.

Equation (1)

$$Y= b_0 + b_1X_1 + b_2X_2 + b_3X_3 + b_{12}X_1X_2 + b_{13}X_1X_3 + b_{23}X_2X_3 + b_{11}X_1^2 + b_{22}X_2^2 + b_{33}X_3^2$$

Table 1: Summary of Variables and their Corresponding Levels in the BBD

Variables utilized for Nano emulsion optimization			
Factors (Independent variables)	**Levels**		
	Low (-1)	**Medium (0)**	**High (+1)**
Oil (%) [X1]	5	7.5	10
S_{mix} (%) [X2]	15	22.5	30
Water (%) [X3]	65	70	75
Responses (Dependent variables)	**Goals**		
Particle size [Y1]	Minimize		
Zeta potential [Y2]	Maximize		
PDI [Y3]	In the range		

Table 2: Independent variables used to generate experimental runs

S. No.	Oil (%) X1	S_{mix} (%) X2	Water (%) X3
1	7.5	22.5	70
2	10	15	70
3	7.5	30	75
4	5	22.5	65
5	7.5	22.5	70
6	5	22.5	75
7	5	15	70
8	10	30	70
9	7.5	15	65
10	7.5	15	75
11	7.5	22.5	70
12	7.5	22.5	70

13	10	22.5	75
14	7.5	30	65
15	5	30	70
16	10	22.5	65
17	7.5	22.5	70

Characterization of Nano emulsion

Particle size, PDI, Zeta potential and Transmission Electron Microscopy (TEM) analysis

The particle size and PDI were assessed using photon correlation spectroscopy, employing the principle of dynamic light scattering (DLS). For the analysis, the nano emulsion samples were diluted 100-fold and evaluated at 25 °C using a Zetasizer (Malvern Instruments Ltd., UK). Each measurement was conducted in triplicate to ensure reliability and reproducibility. (30) Prior to measurement, the samples were diluted 100-fold with double-distilled water and analyzed at 25 °C. All measurements were performed in triplicate to ensure accuracy. In general, zeta potential values beyond ±30 mV are considered indicative of high stability. (31) The morphology of the dispersed phase was characterized by using TEM. For sample preparation, the emulsion was diluted 100 times and sonicated for 2–5 minutes to promote adequate dispersion. A small droplet of the diluted sample was placed on a 300-mesh copper grid and allowed to settle for 1 minute. The grid was then inverted, treated with a drop of phosphotungstic acid (PTA) for 10 seconds, and the excess stain was removed with filter paper. After drying for 4–5 minutes at room temperature, the grid was examined under TEM (JEOL, Mic JEM 1011) (30).

Preparation of NEG

Hydrogels with different strengths were prepared by dissolving GG in purified water under magnetic stirring at 60-70 °C until a transparent mixture was formed. The nanoemulsion was subsequently blended into the gel matrix through slow, dropwise addition, followed by continuous magnetic stirring for at least 30 minutes to achieve homogeneous dispersion.

Preparation of Artificial tear fluid

A simulated tear fluid was formulated by dissolving NaCl (6.78 g), $CaCl_2 \cdot H_2O$ (0.084 g), KCl (1.38 g), and $NaHCO_3$ (2.18 g) in 1000 mL of double-distilled water, and the resulting solution was utilized for subsequent experiments (32).

Characterization of prepared NEG

Sol-Gel transition

Sol to gel transition (gelling capacity) of the formulated gels was evaluated by mixing the gel with simulated tear fluid in a 4:1 ratio and maintaining the temperature at 34 ± 0.5 °C to mimic physiological conditions. The gelling capacity and time were then assessed by visual observation as codified in Table 3.

Table 3: Coding for Gelling capacity

Coding	Observation
-	Absence of gel formation
+	Gel formation initiates within minutes and sustains for a brief period (1-2 hrs)
++	Rapid onset of gelation (within 30 seconds) persisting for several hours (4-5 hrs)
+++	Swift gelation (within 30 seconds) with long-term stability (indefinite duration)
++++	Instant gel formation resulting in a highly rigid and enduring structure

Viscosity and Rheological studies

Brookfield viscometer was used to determine the viscosity of prepared formulations. Each formulation was transferred to an appropriate container, and its viscosity was first measured with spindle No. 64 prior to the addition of artificial tear fluid. Afterward, simulated tear fluid was incorporated into the samples, and viscosity was again assessed using the suitable spindle. Measurements were taken at various rotational speeds, and the most appropriate speed was selected for final data recording (32). The rheology of the selected formulation was measured using by rotational viscometer, and the results were recorded.

pH measurement

The pH value represents a key parameter in eye drop formulations, with an optimal range of 5 to 7.4 to ensure compatibility. Each formulation's pH was determined with a digital pH meter, which had been validated at 25°C against buffer solutions at pH 4, 7, and 10 prior to evaluation. Determinations were performed in triplicate, and the mean results were recorded (33).

Drug content determination

To evaluate the drug concentration in the refined formulation, 1 mL of the sample was first diluted with methanol to reach a total volume of 10 mL within a volumetric flask. This diluted solution was subsequently moved to a centrifuge tube and subjected to centrifugation at 7000 rpm for 1 hour at 4 °C, promoting full separation and disruption of the dispersed components. The clear supernatant layer produced was

afterward analysed using HPLC for accurate quantification.

Sterility Testing

All formulation components were sterilized by autoclaving before preparation. The entire process was conducted under a laminar airflow cabinet to ensure aseptic handling. After filling and sealing, the containers were exposed to UV light for surface sterilization to reduce the possibility of cross-contamination during further testing. The sterility of the samples was evaluated using the direct inoculation technique. In this procedure, 1 mL of each formulation was aseptically introduced into two separate culture media—fluid thioglycolate medium (50 mL) and soybean–casein digest medium (50 mL). The thioglycolate medium was maintained at 30–35 °C and the soybean–casein medium at 20–25 °C for a 14-day incubation period. Throughout this time, both media were regularly examined for any visible indications of microbial contamination (3).

Isotonicity

Since ophthalmic preparations must be non-irritating and safe for ocular tissues, isotonicity represents a critical evaluation parameter. A blood sample was procured from an authorized blood bank. To assess isotonicity, the formulation was mixed with a few drops of fresh blood and examined microscopically at 45× magnification. The red blood cells (RBCs) were observed for morphological changes, where the absence of shrinkage or swelling indicated isotonic compatibility of the formulation (34).

***In vitro* drug release**

The in vitro release kinetics of the drug were investigated employing the dialysis membrane diffusion technique. Prior to experimentation, a dialysis tubing featuring a 10 kDa molecular weight cutoff was equilibrated by immersion in artificial tear solution for a full night. The dissolution environment comprised 20 ± 0.5 mL of newly prepared artificial tear solution. Within the dialysis pouch, 1 mL of the prepared formulation was introduced alongside 50 µL of artificial tear solution. To replicate physiological eye temperature, the apparatus was held constant at 35 ± 0.5 °C while undergoing gentle magnetic stirring at 50 rpm. At designated sampling points (0.5, 1, 2, 4, 6, 8, and 24 hours), 2 mL portions were sampled from the medium and immediately replenished with an equivalent amount of fresh artificial tear solution to preserve sink conditions throughout. The levels of bimatoprost in these withdrawn portions were assayed via high-performance liquid chromatography (HPLC) according to an established protocol. Ultimately, the release kinetics were visualized through a graph depicting the cumulative drug release percentage as a function of elapsed time (28).

Release kinetics

To interpret the in vitro drug release profiles, various kinetic models were employed to characterize the release mechanism. Assessing release kinetics provides insight into the rate and duration of drug action, helping to predict its therapeutic performance.

Stability Studies

Stability testing was conducted for a period of three months at 4 °C ± 1 °C, ambient conditions (25 °C ± 1 °C), and 40 °C ± 1 °C in accordance with ICH Q1(A) guidelines for Zone III. The formulations were stored in airtight containers, and samples were periodically collected to assess appearance, particle size, zeta potential, in situ gelation properties, and drug content (28).

Pharmacodynamic studies

All animal studies were conducted in compliance with the CPCSEA (Committee for the Purpose of Control and Supervision of Experiments on Animals) norms and the ARVO guidelines governing the ethical use of animals in ophthalmic and vision research. The study design was reviewed and approved by the Institutional Animal Ethics Committee (IAEC), with the assigned reference CPCSEA/IAEC/12/2024/24. Healthy albino rabbits from the New Zealand strain (weighing 2.0–2.5 kg) were chosen for the research and maintained in separate enclosures within a controlled facility environment, including a stable temperature of 25 ± 0.5 °C, humidity levels of 55 ± 1%, and a 12:12-hour light-dark regimen. The rabbits received unlimited supplies of a well-formulated commercial feed and clean, filtered water. To facilitate adjustment to the lab setting, all subjects completed a seven-day habituation period before any procedures began.

Grouping, induction of glaucoma and treatment

Rabbits with baseline intraocular pressure (IOP) from 15.5 to 17 mmHg were chosen and divided randomly into four groups, with each group containing six subjects. Group I served as the untreated healthy control and received no interventions during the entire experiment. In Groups II, III, and IV, glaucoma was induced in the right eye through the application of 0.1% dexamethasone (DEX) eye drops four times per day over a 28-day period. To prevent IOP from returning to normal levels—which

could occur within one week after stopping DEX—the treatment was maintained to keep the elevated pressure ongoing. After confirming a stable IOP elevation at the end of week four, the application was adjusted to twice daily. Post-induction, Group II remained without additional interventions and acted as the untreated glaucoma control. Starting on day 30 and continuing until day 60, however, Groups III and IV underwent treatment protocols. Subjects in Group III got one daily drop of the commercial product Lumigan®, while those in Group IV were given one daily dose of the experimental nano formulation (FX). IOP readings were obtained on days 28, 42, and 60, consistently employing the identical measurement technique **(Fig 1)**.

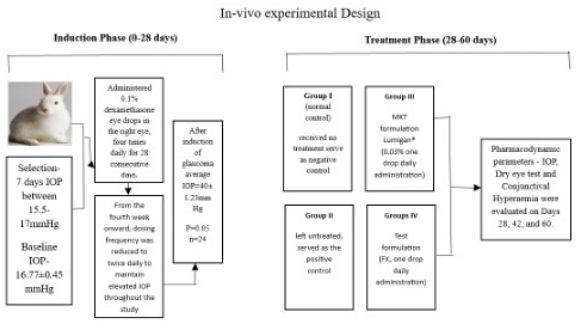

Fig 1: *In vivo* experimental design for pharmacodynamic evaluation

Evaluation parameters

IOP measurement

A calibrated tonometer was used to measure IOP under controlled conditions. For every individual eye, three readings were recorded, and the average value was used to ensure reliable measurements.

Dry eye test

Tear secretion was measured using the Schirmer tear test, which is a standard procedure for evaluating lacrimal gland activity and identifying dry eye conditions. Schirmer test strips were carefully inserted into the lower eyelid (conjunctival fornix) of the treated eye, taking care to avoid stimulating reflex tearing. The strips were kept in place for a duration of five minutes, after which the wetted length was measured in millimeters with the help of a calibrated ruler. All assessments were carried out under controlled environmental conditions to avoid factors such as airflow or bright light that could affect tear production.

Conjunctival hyperemia

Ocular surface inflammation was assessed using slit-lamp biomicroscopy along with a standardized 10-point grading scale to maintain uniformity and accuracy. Scores between 0 and 3 indicated minimal inflammation or slight conjunctival redness, 4 to 6 reflected mild to moderate hyperaemia, 7 to 8 represented moderate to marked inflammation, and 9 to 10 signified severe conjunctival hyperaemia. All evaluations were conducted by an examiner who was masked to the treatment groups to prevent observer bias.

All results were expressed as mean ± standard deviation. Statistical comparisons were carried out using one-way ANOVA, followed by Tukey's post hoc test or Student's paired t-test, wherever applicable.

Results and Discussion

Characterization of optimized nano emulsion

Development of nano emulsion formulations using Box-Behnken design

Employing a Box-Behnken experimental setup with three independent variables, each tested at three levels, resulted in the development and evaluation of 17 distinct nano emulsion formulations targeting key response parameters. Across the experimental trials, droplet size (Y1) values fluctuated between 22.17 ± 0.43 nm and 44.97 ± 0.36 nm, zeta potential (Y2) spanned from –14.7 ± 0.48 mV to –36.47 ± 0.35 mV, and polydispersity index (Y3) ranged from 0.106 ± 0.014 to 0.248 ± 0.001, with details outlined in Table 4. The response data from these 17 formulations were subjected to regression analysis via linear, two-factor interaction, and quadratic polynomial equations. Of the options evaluated, the quadratic equation yielded the most robust fit, confirmed by its statistical significance ($p < 0.05$) (Table 5)

Table 4: BBD with independent variables and obtained responses

S. No.	Independent Variables			Dependent Variables					
	Oil (%) X1	Smix (%) X2	Water (%) X3	**Actual Particle size (nm) Y1	*Predicted Particle size (nm) Y1	**Actual Zeta Potential (mV) Y2	*Predicted Zeta Potential (mV) Y2	**Actual PDI Y3	*Predicted PDI Y3

1	7.5	22.5	70	22.17±0.43	22.24	-36.4±0.55	-36.33	0.122±0.004	0.122
2	10	15	70	31.82±0.56	32.01	-18.68±0.45	-18.5	0.241±0.076	0.240
3	7.5	30	75	42.35±0.37	42.33	-16.1±0.56	-16.08	0.201±0.005	0.201
4	5	22.5	65	25.31±0.58	25.33	-18.6±0.78	-18.66	0.106±0.014	0.105
5	7.5	22.5	70	22.15±0.64	22.24	-36.47±0.35	-36.33	0.123±0.065	0.122
6	5	22.5	75	28.12±0.72	28.33	-24.7±0.63	-24.54	0.114±0.003	0.113
7	5	15	70	29.65±0.28	29.6	-26.9±0.84	-26.81	0.129±0.006	0.129
8	10	30	70	44.97±0.36	45.02	-19.5±0.66	-19.59	0.248±0.001	0.247
9	7.5	15	65	32.75±0.73	32.77	-15.5±0.46	-15.52	0.174±0.009	0.174
10	7.5	15	75	37.8±0.39	37.63	-23.9±0.44	-24.15	0.178±0.011	0.178
11	7.5	22.5	70	22.18±0.22	22.24	-36.18±0.86	-36.33	0.122±0.020	0.122
12	7.5	22.5	70	22.46±0.44	22.24	-36.24±0.36	-36.33	0.123±0.005	0.122
13	10	22.5	75	39.76±0.77	39.74	-21.2±0.90	-21.13	0.226±0.002	0.226
14	7.5	30	65	38.47±0.15	38.64	-14.7±0.48	-14.45	0.178±0.017	0.177
15	5	30	70	27.35±0.49	27.16	-16.4±0.88	-16.58	0.146±0.013	0.1469
16	10	22.5	65	34.4±0.33	34.19	-16.6±0.50	-16.76	0.204±0.003	0.2049
17	7.5	22.5	70	22.25±0.81	22.24	-36.35±0.87	-36.33	0.123±0.022	0.1226

[**]Actual Particle Size-Particle size analyzed after development of formulation experimentally, [*]Predicted particle size- Particle size predicted by the software after addition of results in software.

Table 5: Anova results for responses obtained from experimental design response

Model Fit parameters	Y1: Particle Size			Y2: Zeta Potential			Y3: PDI		
	F value	P value	Interpretation	F value	P value	Interpretation	F value	P value	Interpretation
Model (Quadratic)	2567.59	< 0.0001	Significant	2875.82	< 0.0001	Significant	5168.38	< 0.0001	Significant

X_1	4957.68	< 0.0001	Significant	307.84	< 0.0001	Significant	28863.12	< 0.0001	Significant
X_2	13466.88	< 0.0001	Significant	912.06	< 0.0001	Significant	417.59	< 0.0001	Significant
X_3	882.94	< 0.0001	Significant	1147.04	< 0.0001	Significant	521.63	< 0.0001	Significant
X_1X_2	1441.54	< 0.0001	Significant	699.51	< 0.0001	Significant	32.11	0.0008	Significant
X_1X_3	39.27	0.0004	Significant	12.28	0.0099	Significant	62.94	< 0.0001	Significant
X_2X_3	8.27	0.0238	Significant	267.48	< 0.0001	Significant	115.92	< 0.0001	Significant
X_1^2	703.66	< 0.0001	Significant	402.49	< 0.0001	Significant	3134.52	< 0.0001	Significant
X_2^2	747.928	< 0.0001	Significant	802.29	< 0.0001	Significant	1062.516	< 0.0001	Significant
X_3^2	501.984	< 0.0001	Significant	818.691	< 0.0001	Significant	1354.33	< 0.0001	Significant
Lack of fit	4.6	0.0872	Not significant	6.37	0.0528	Not significant	4.72	0.0839	Not significant
Predicted R^2	0.9961			0.9963			0.9981		
Adjusted R^2	0.9993			0.9994			0.9997		
Adequate Precision	145.93			133.27			209.82		

Effects of independent factors on Particle Size

The ANOVA results (Table 5) for the quadratic model demonstrated that the model was highly significant, with an overall F-value of 2567.59 ($p < 0.0001$), indicating that the selected formulation variables effectively explain the variation in particle size. Among the main effects, oil (X_1), Smix (X_2), and water (X_3) were all highly significant ($p < 0.0001$), confirming their strong influence on particle size. The interaction effects were also significant, with the X_1 X_2 interaction (oil × Smix) exerting the most pronounced effect ($F = 1441.54$, $p < 0.0001$), followed by X_1 X_3 (oil × water) ($F = 39.27$, $p = 0.0004$) and X_2 X_3 (Smix × water) ($F = 8.27$, $p = 0.0238$). Furthermore, the quadratic terms (X_1^2, X_2^2, and X_3^2) were highly significant ($p < 0.0001$), suggesting strong curvature effects and confirming the non-linear relationship of each factor with particle size. The lack of fit was found to be statistically non-significant ($F = 4.60$, $p = 0.0872$), suggesting an adequate model fit. The Predicted R^2 (0.9861) was in close agreement with the Adjusted R^2 (0.9993), with a difference of less than 0.2, confirming good model predictability. The Adequate Precision value of 145.93, far exceeding the threshold of 4, further indicates a strong signal-to-noise ratio and suitability of the model for design space exploration.

Smix concentration exhibited a non-linear effect on particle size, where an initial increase reduced particle size, but further increase led to larger droplets. This can be attributed to excess surfactant molecules aggregating in the continuous phase, reducing stabilization efficiency and resulting in incomplete oil droplet coverage. In contrast, variations in oil and water concentration had no significant impact on particle size **(Fig 2)**.

Equation 2,

$$\text{Particle size}=22.242+5.065X_1+2.64X_2+2.1375X_3+3.8625X_1X_2+0.6375X_1X_3-0.2925X_2X_3+2.63025X_1^2+8.57525X_2^2+7.02525X_3^2$$

Effects of independent factors on Zeta Potential

The quadratic model for zeta potential was highly significant ($F = 2875.82$, $p < 0.0001$), indicating strong influence of formulation factors. oil (X_1), Smix (X_2), and water (X_3) all showed significant effects, with Smix and water being more dominant. Interaction terms X_1 X_2 and X_2 X_3 were highly significant, while X_1 X_3 had a weaker but notable effect. Strong quadratic effects (X_1^2, X_2^2, and X_3^2) confirmed non-linear factor relationships. Minimal residual error and a non-significant lack of fit ($p = 0.0528$) suggest good model adequacy. The Predicted R^2 value of 0.9963 was in close agreement with the Adjusted R^2 value of 0.9994, with a difference of less than 0.2, indicating strong model reliability. An Adeq Precision value of 133.27 confirmed an excellent signal-to-noise ratio, demonstrating that the model is appropriate for navigating the design space. The results showed that increasing the Smix concentration initially led to a rise in the zeta potential of the nano emulsions; however, beyond a certain point, further increases in Smix caused a decline in zeta potential. In contrast, changes in the oil and water levels did not exhibit any notable influence on zeta potential.

Equation 3,

$$\text{Zeta potential} = -36.328+1.3275X_1+2.285X_2-2.5625X_3-2.83X_1X_2+0.375X_1X_3+1.75X_2X_3+6.6165X_1^2+9.3415X_2^2+9.4365X_3^2$$

Effects of independent factors on PDI

The quadratic model for PDI was highly significant ($F = 5168.38$, $p < 0.0001$), confirming a strong influence of formulation variables. oil (X_1), Smix (X_2), and water (X_3) all had significant effects, with oil showing the most dominant contribution. Interaction terms (X_1 X_2, X_1 X_2, X_2 X_3) were also significant, indicating combined effects of factors. Additionally, strong quadratic contributions (X_1^2, X_2^2, and X_3^2) highlighted non-linear relationships. The residual error was minimal, and the lack of fit was not significant ($p = 0.0839$), confirming good model adequacy. The Predicted R^2 value of 0.9981 closely matched the Adjusted R^2 value of 0.9997, with a difference of less than 0.2, indicating strong model reliability. Adequate Precision, which evaluates the signal-to-noise ratio and should be greater than 4, was recorded as 209.82, confirming an excellent and highly acceptable signal. These results demonstrate that the model is well-suited for exploring and interpreting the design space.

Equation 4,

$$\text{PDI} = 0.1226+0.053X_1+0.006375X_2+0.007125X_3-0.0025X_1X_2+0.0035X_1X_3+0.00475X_2X_3+0.024075X_1^2+0.044325X_2^2+0.015825X_3^2$$

Numerical optimization was applied to identify the most suitable nano emulsion formulation. The optimized composition was determined by evaluating how the independent variables influenced the measured responses. Optimization criteria were established by specifying the acceptable ranges and desired targets for each factor.

The optimized levels of X1 and X2 were identified as 7.5% and 22.5% respectively, as shown in the desirability plot (Fig. 3). This plot outlines the most favorable conditions required to obtain the desired particle size, zeta potential, and PDI, yielding an overall desirability value of 1.

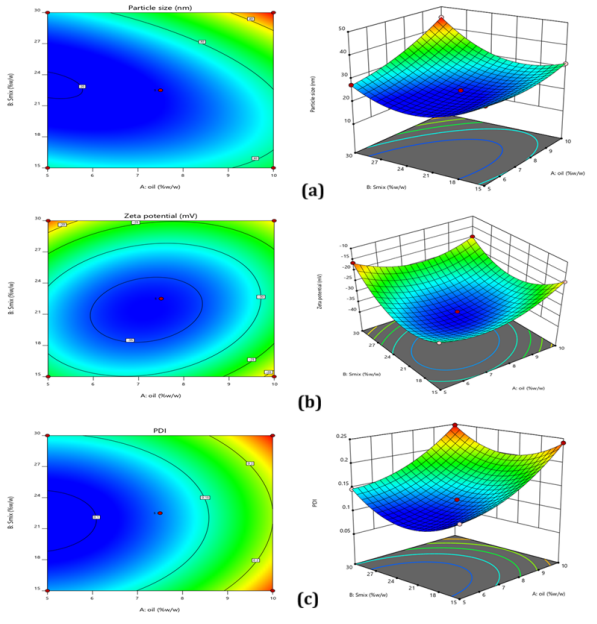

Fig 2: Model-predicted response surface and contour plots for (a) particle size, (b) zeta potential, and (c) PDI using the QbD approach

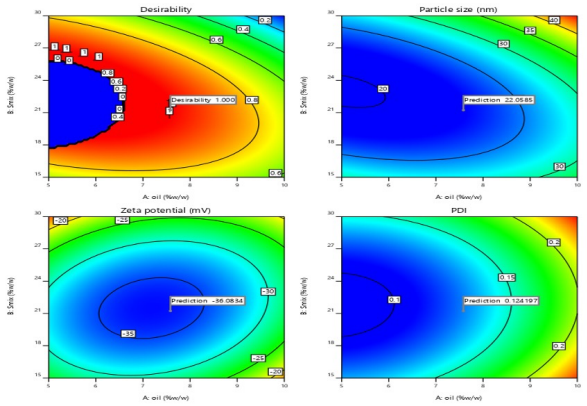

Figure 3: QbD-Based Desirability Profiles for Optimizing Particle Size, Zeta Potential, and PDI

The optimized nanoemulsion met the targeted nanoscale size, showed a low PDI, and possessed a high enough zeta potential to maintain stability and minimize particle aggregation. Since the stability of colloidal systems is largely governed by their zeta potential, these findings indicate good formulation robustness. As presented in Table 6, the predicted responses closely matched the experimental outcomes ($p > 0.05$), confirming the reliability of the Design Expert software and demonstrating that the applied design methodology effectively produced nanoemulsions with the intended characteristics.

Table 6: Predicted vs. Actual Results for the Optimized Nano emulsion Formulation

Optimized formula	Optimized level	Responses	Predicted value	Experimental value	P value
Oil (%)	7.5	Particle Size (nm)	22.24±0.20	22.17±0.91	0.907
S_{mix} (%)	22.5	Zeta potential (mV)	-36.32±0.21	-36.40±0.34	0.750
Water (%)	70	PDI	0.122±0.00088	0.123±0.04	0.969

Particle size, PDI, Zeta potential and TEM analysis

The particle size and distribution profile of the optimized nano emulsion are depicted in **Fig 4**. The average droplet size measured was 22.17±0.91nm, accompanied by a low polydispersity index of 0.123±0.04, indicating a narrow size distribution. The zeta potential was determined to be -36.4 ± 0.98 mV, suggesting that the nano emulsion carries a negative surface charge, which typically correlates with enhanced physical stability (Figure 3b). To further examine the droplet morphology and dispersion characteristics, TEM analysis was performed. The results revealed that the droplets in the optimized formulation were uniformly spherical, with sizes ranging from 30 to 53 nm **(Fig 5).**

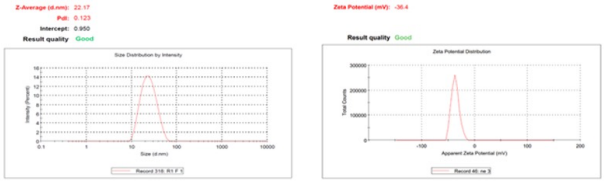

Fig 4: Characterization of optimized nano emulsion (a) Particle size distribution and (b) Zeta potential

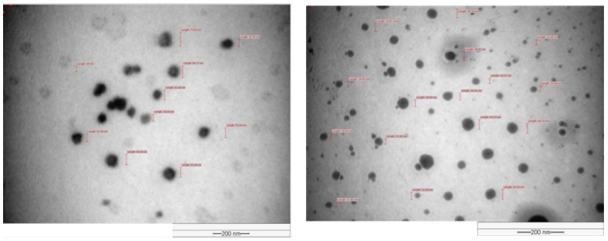

Fig 5: TEM images of optimized nano emulsion at 200nm magnification

NEG characterization

Following incorporation of the nanoemulsion into the hydrogel, the resulting NEG was evaluated for various parameters. The formulation was clear, transparent, and free from turbidity or foreign particles **(Fig 6)**.

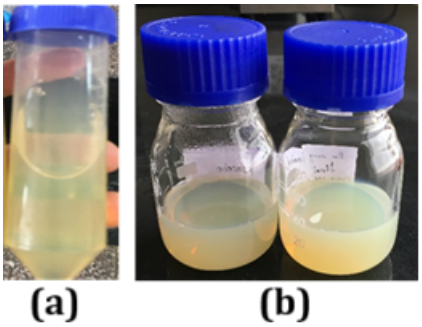

Fig 6: Prepared formulations (a) Nano emulsion (b) NEG (After incorporation into hydrogel base)

Sol-gel transition/Gelling capacity

Gelling capacity was assessed as described in Table 3, with results summarized in Table 7. At low concentrations (NEG A), gelation occurred after 3–5

minutes and persisted for 2–4 hours. Increasing the concentration reduced gelation time and extended gel duration. Moderate concentration (NEG B) resulted in immediate gelation with prolonged retention, while high concentration (NEG C) produced immediate but very stiff gels **(Fig 7)**.

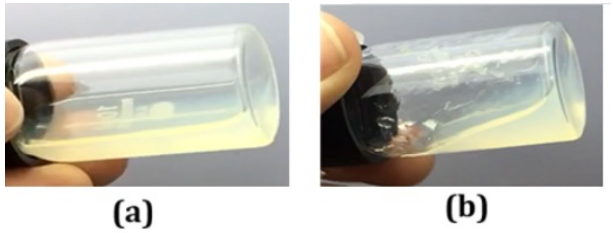

Fig 7: Sol-gel transition of NEG formulation (a) without tear fluid and (b) with tear fluid

Table 7: Characterization of developed gels for appearance, viscosity and Gelling capacity

Formulation	GG (%)	Before gelation Viscosity (Pa.s)	After gelation viscosity (Pa.s)	Appearance	Gelling capacity
NEG A	0.125%	49.5 ±1.25	428±2.10	Transparent	+
NEG B	0.250%	55.1± 1.00	1350± 1.65	Transparent	+++
NEG C	0.5 %	77.9± 1.30	5600± 1.80	Transparent	++++

Viscosity and Rheological behavior

Viscosity is critical in ocular drug delivery, as it affects gel residence time in the precorneal region. Viscosity results before and after gelation are presented in Table 7 and **Fig 8**.

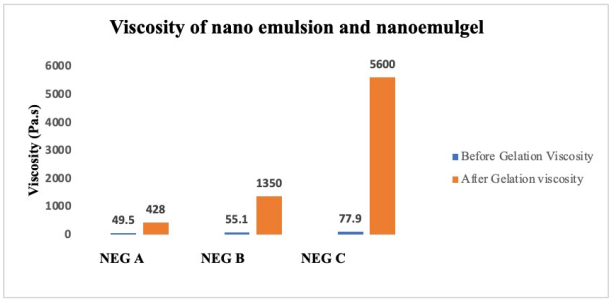

Fig. 8: Viscosity of developed NEG without tear fluid (Viscosity before gelation) or NEG with tear fluid (Viscosity after gelation)

An increase in viscosity helps extend the residence time of the gel, supporting sustained drug release. Nevertheless, excessively high viscosity can hinder blinking and impair vision. For this reason, formulations exhibiting pseudoplastic behavior are preferred, as they provide a suitable compromise between prolonged retention and user comfort. Considering both viscosity and gelling capacity, NEG B was identified as the optimal formulation and was subsequently subjected to further assessments, including rheological analysis, drug content, pH, sterility, isotonicity, and in vitro release studies. The rheogram of the optimized gel is presented in Figure 9. Gellan gum–based gels show pseudoplastic flow, in which viscosity decreases under higher shear conditions—such as blinking—and increases when shear stress is minimal. This shear-dependent behavior promotes ease of instillation while maintaining extended precorneal retention, ultimately supporting better patient comfort and treatment adherence. **(Fig 9)**.

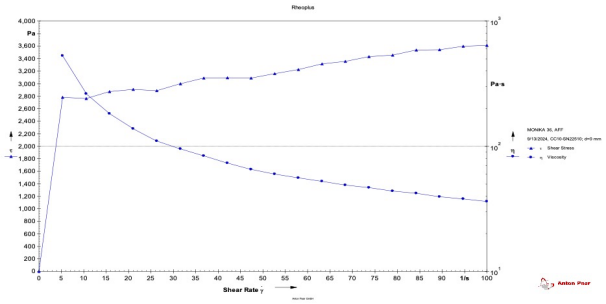

Fig 9: Rheological behavior of optimized NEG formulation

pH measurement

The optimized formulation exhibited a pH of 7.14 ± 0.40, which falls well within the acceptable ocular pH range of 5–7.4. This indicates that the formulation is appropriate and safe for ophthalmic administration.

Drug content

Drug content denotes the quantity of active pharmaceutical ingredients (API) contained within a formulation, serving as a measure of uniformity and reliability in therapeutic dosing. The observed value of drug content was 98.76±0.54% in final optimized NEG.

Sterility testing

After incubation, no microbial growth was detected in the sterilized NEG, confirming the formulation's sterility.

Isotonicity

The findings (Fig. 10) show that the optimized formulation (NEG-B) is isotonic and does not induce osmotic damage to red blood cells, confirming its suitability for ocular use and its potential to maintain comfort and safe.

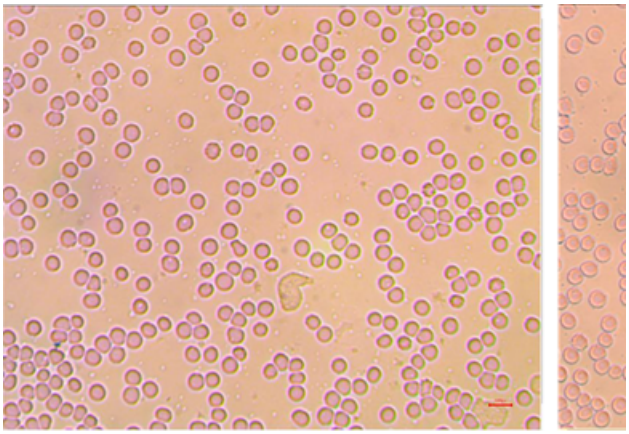

(a)

Fig 10. Isotonicity study of NEG formulation using RBC in normal saline (a) and RBC in optimized NEG formulation

In-Vitro Drug Release

In vitro release testing was performed in simulated tear fluid using a diffusion-based setup. The release profiles of the optimized NEG formulation and the pure drug are presented in Figure 10. The plain drug exhibited a rapid release, with 85.25% diffusing out within the first 4 hours. In contrast, the optimized NEG displayed an initial burst release followed by a gradual, extended-release period, attributed to nanodroplets present on the gel surface. By 24 hours, the formulation achieved a cumulative release of 91.29%, demonstrating its sustained-release capability. These results confirm that the NEG system provides controlled and prolonged delivery of bimatoprost (Fig. 11).

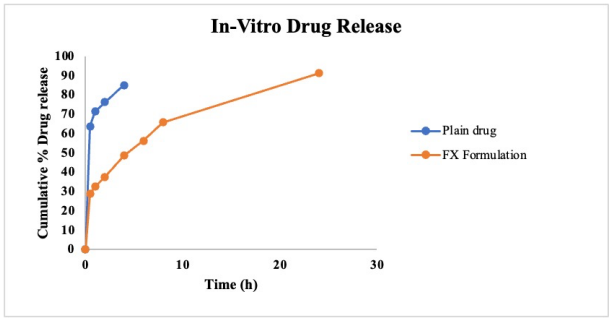

Fig 11: ***In vitro*** **drug release profile of bimatoprost from developed NEG**

Release Kinetics

The drug-release data were fitted to several kinetic models, including zero-order, first-order, Higuchi, Korsmeyer–Peppas, and Hixson–Crowell to characterize the release mechanism of developed and optimized NEG formulation. Comparison of the correlation coefficients revealed that the first-order model showed a noticeably better fit than the zero-order model, with R^2 values of 0.9796 and 0.7598, respectively. The Higuchi model produced an R^2 of 0.9533, while the Korsmeyer–Peppas model showed an R^2 of 0.9788. The highest correlation was observed with the Hixson–Crowell model (R^2 = 0.9847), as summarized in Table 8. This strong correlation indicates that the release mechanism is governed primarily by changes in the surface area and geometry of the formulation, suggesting erosion or dissolution-based release rather than simple diffusion (Fig. 12).

Table 8: R^2 value for applied kinetic models

Kinetic Models	R^2
Zero order	0.7598
First order	0.9796
Higuchi model	0.9533
K-P model	0.9788
Hixson-Crowell model	**0.9847**

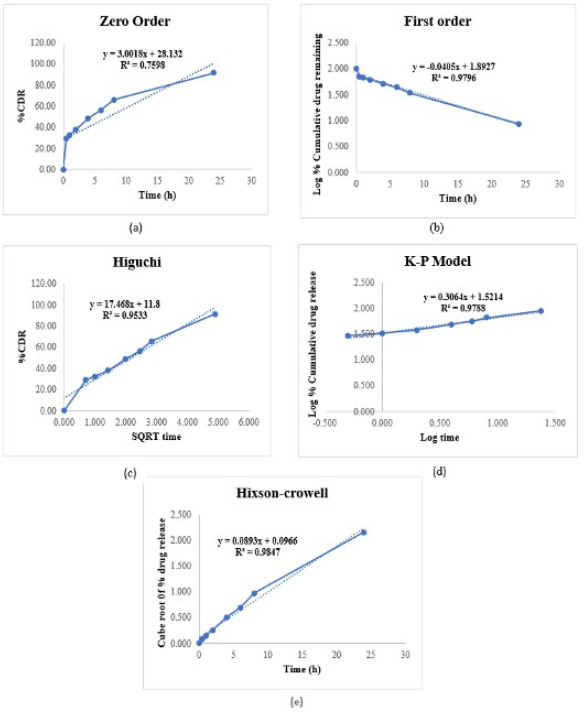

Fig 12: Mathematical models (a) zero order kinetics, (b) First order kinetics, (c) Higuchi model, (d) K-P model and (e) Hixson-Crowell model

Stability studies

Throughout the study, samples were routinely assessed for key stability indicators summarized in Table 9. The NEG was specifically examined for attributes including visual transparency, droplet dimensions, surface charge, gel formation ability, and active ingredient uniformity to gauge its long-term robustness.

The NEG preserved its transparent appearance across all tested environmental conditions, signaling no evidence of structural breakdown. Droplet size showed minimal variation at refrigerated temperatures (4 °C), rising slightly from 22.67 ± 0.74 nm to 24.16 ± 0.86 nm without reaching statistical relevance. Under ambient conditions (25 °C), dimensions grew from 22.69 ± 0.78 nm to 26.64 ± 0.69 nm, with notable differences emerging by the second and third months ($p < 0.001$). Elevated heat (40 °C) prompted a sharper escalation, from 22.80 ± 0.83 nm to 28.86 ± 0.56 nm, achieving significance from the second month onward ($p < 0.001$), which points to heat-induced clustering of particles. Surface charge held steady in the cold (4 °C), shifting nonsignificantly from -36.4 ± 0.72 mV to -35.98 ± 0.98 mV. However, it declined markedly at 25 °C (from -36.46 ± 0.73 mV to -33.97 ± 0.75 mV; $p < 0.05$ by month 2, $p < 0.001$ by month 3) and even more so at 40 °C (from -36.78 ± 0.91 mV to -33.14 ± 0.83 mV; $p < 0.001$ from month 2 onward), reflecting diminished dispersion stability—yet levels stayed sufficiently negative to support overall integrity. Gel formation strength remained robust and unchanged (rated +++ in all cases). Active ingredient levels were largely consistent at 4 °C (from 98.76 ± 0.54% to 98.62 ± 0.44%, nonsignificant), accompanied by only trivial, insignificant dips under warmer storage at 25 °C and 40 °C. The data underscore optimal performance at 4 °C, where minimal disruptions occurred, whereas higher temperatures triggered pronounced shifts in droplet size and charge, underscoring refrigeration as the ideal preservation strategy.

Table 9: Stability studies Data of developed NEG in the observation period

Months	Temperature (°C)	Clarity	Particle size (nm)	Zeta potential (mV)	Gelling capacity	% Drug Content
0	4°C±1 °C	Clear solution	22.67 ±0.74	-36.4± 0.72	+++	98.76 ±0.54
	25°C± 1°C	Clear solution	22.69 ±0.78	-36.46 ±0.73	+++	98.54 ±0.36
	40°C± 1°C	Clear solution	22.80 ±0.83	-36.78 ±0.91	+++	98.35 ±0.28
1	4°C±1 °C	Clear solution	22.94 ±0.69 ^{a1} **ns**	-35.48 ±0.62 ^{a1} **ns**	+++	98.63 ±0.87 ^{a1} **ns**
	25°C± 1°C	Clear solution	23.81 ±0.87 ^{b1}**ns**	-35.46 ±0.54 ^{b1*}	+++	98.35 ±0.49 ^{b1}**ns**
	40°C± 1°C	Clear solution	23.99 ±0.88 ^{c1}**ns**	-34.31 ±0.86 ^{c1***}	+++	97.84 ±0.58 ^{c1}**ns**
2	4°C±1 °C	Clear solution	23.89 ±0.53 ^{a1} **ns**	-35.42 ±0.78 ^{a2}**ns**	+++	98.63 ±0.64 ^{a2}**ns**
	25°C± 1°C	Clear solution	24.49 ±0.85 ^{b2***}	-34.90 ±0.28 ^{b2**}	+++	98.84 ±0.77 ^{b2}**ns**
	40°C± 1°C	Clear solution	25.77 ±0.87 ^{c2***}	-34.02 ±0.76 ^{c2***}	+++	97.45 ±0.62 ^{c2}**ns**

3	4°C±1°C	Clear solution	24.16 ±0.86 ^{a1} **ns**	-35.98 ±0.98 ^{a3}**ns**	+++	98.62 ±0.44 ^{a3}**ns**
	25°C± 1°C	Clear solution	26.64 ±0.69 ^{b3***}	-33.97 ±0.75 ^{b3***}	+++	98.12 ±0.37 ^{b3}**ns**
	40°C± 1°C	Clear solution	28.86 ±0.56 ^{c3***}	-33.14 ±0.83 ^{c3***}	+++	97.14 ±0.85 ^{c3}**ns**

Statistical analysis of data was carried by one-way ANOVA followed by Tukey's Multiple Range Test. The values are Mean ± SD for each group (n=3). For 4°C the coding is ^{a1}Zero-month v/s 1st month, ^{a2}Zero-month v/s 2nd month, ^{a3}Zero-month v/s 3rd month, for 25°C the coding is ^{b1}Zero-month v/s 1st month, ^{b2}Zero-month v/s 2nd month, ^{b3}Zero-month v/s 3rd month, for 40°C the coding is ^{c1}Zero-month v/s 1st month, ^{c2}Zero-month v/s 2nd month, ^{c3}Zero-month v/s 3rd month. (* p<0.05, ** p<0.01, *** p<0.001, ns-non-significant).

Pharmacodynamic studies

IOP

IOP remained stable in the normal group (16–17 mmHg) throughout the study. The disease control group showed a progressive elevation, reaching 49.17 ± 1.17 mmHg at day 60. The marketed formulation (Lumigan) demonstrated a significant reduction in IOP compared to the disease control group from day 42 onward ($p < 0.001$), with values declining to 19.50 ± 2.26 mmHg by Day 60. The test formulation (FX) also significantly reduced IOP versus the disease control ($p < 0.001$) but showed comparatively higher values than Lumigan (23.67 ± 2.88 mmHg at day 60; $p < 0.01$– 0.001 vs. Lumigan) (Table 10, **Fig. 13a**). These findings are in agreement with previous reports that prostaglandin analogues such as bimatoprost (Lumigan®) effectively reduce IOP by enhancing uveoscleral outflow (35). The FX formulation also demonstrated effective IOP-lowering potential, likely due to the combined pharmacological effects of its components, aligning with earlier studies reporting synergistic IOP reduction by novel nano formulations (36).

Dry eye test

Schirmer's test values remained consistent in the normal and disease control groups, indicating stable tear production. The marketed formulation caused a significant decline in tear secretion at both day 42 and day 60 ($p < 0.001$), whereas the test formulation showed a comparatively milder reduction, with non-significant change at day 42 and a moderate but significant decline at day 60 ($p < 0.001$ vs. disease control) (Table 10, **Fig.13b**). This observation is consistent with the literature reporting that long-term use of prostaglandin analogues can disrupt tear film stability and induce ocular surface dryness (37,38). The FX formulation's incorporation of hyaluronic acid (HA) and omega-3 fatty acids likely contributed to maintaining tear stability, as both have been reported to improve ocular surface lubrication and mitigate dry eye symptoms (39,40)

Conjunctival hyperemia

Conjunctival hyperemia scores were minimal in the normal group (0) but increased slightly in the disease control. Lumigan caused a pronounced rise in hyperemia scores at Day 42 (5.83 ± 0.75; $p < 0.001$) and day 60 (7.17 ± 0.75; $p < 0.001$). By contrast, the test formulation produced significantly lower hyperemia scores at both time points compared with Lumigan (day 42: 4.10 ± 1.05, $p < 0.01$; day 60: 4.60 ± 0.75, $p < 0.001$), indicating a better tolerability profile. (Table 10, **Fig 13c**). This is supported by earlier studies showing that prostaglandin analogues frequently induce conjunctival hyperemia due to vasodilation mediated by FP receptor stimulation (41,42). The reduced incidence of hyperaemia in the FX group suggests better tolerability, likely attributable to the biocompatible excipients and controlled drug release profile of the test nano formulation **(Fig 14)**.

Table 10: Pharmacodynamic comparison between disease control group and anti-glaucoma therapy groups (MKT formulation group and test formulation group)

Test parameter	Time (Days)	Normal group	Disease Control	MKT Formulation (Lumigan)	FX treatment (Test formulation)
IOP (mm Hg)	**28th day**	16.83±1.17	39.50±1.87	39.17±2.93 $^{a-ns}$	39.00±2.61 $^{b-ns, c-ns}$
	42nd day	16.50±1.05	41.83±1.94	30.33±2.16 $^{a-***}$	35.17±2.23 $^{b-***, c-**}$

	60th day	17.00±1.10	49.17±1.17	19.50±2.26 a-***	23.67±2.88 b-***, c-**
Schiemer's Test (mm/5min)	**28th day**	9.83±0.75	9.33±0.52	9.67±1.21 a-ns	10.00±1.26 b-ns, c-ns
	42nd day	10.17±1.17	9.83±0.75	6.67±1.21 a-***	8.33±0.82 b-ns, c-*
	60th day	10.17±1.17	9.67±0.82	5.33±0.82 a-***	7.17±0.75 b-***, c-*
Conjunctival hyperemia (grading -0-10)	**28th day**	**0-Noredness, clear conjunctiva, no swelling, no discharge, clear anterior chamber**	3.00±0.89	3.17±0.75 a-ns	3.33±0.82 b-ns, c-ns
	42nd day		3.50±0.55	5.83±0.75 a-***	4.10±1.05 b-ns, c-**
	60th day		3.33±0.52	7.17±0.75 a-***	4.60±0.75 b-*, c-***

Statistical analysis of data was carried by one-way ANOVA followed by Tukey's Multiple Range Test. The values are Mean ± SD for each group (n=6). [a]Disease control v/s MKT, [b]Disease control v/s FX, [a]MKT v/s FX. (* $p<0.05$, ** $p<0.01$, *** $p<0.001$, ns-non-significant) (The normal group, disease control and marketed formulation was common for two formulations i.e. FX and already publish FF formulation) (43)

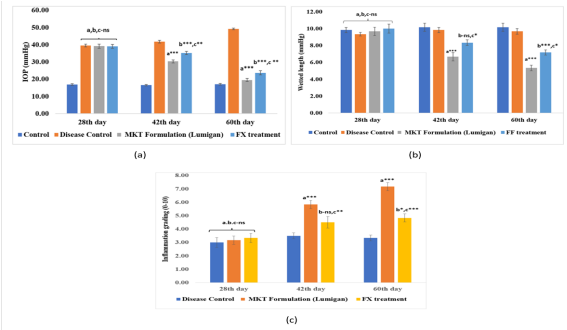

Fig 13: *In vivo* analysis for IOP, Dry eye test and conjunctival hyperemia (a)IOP measurement of negative control (normal saline), positive control, MKT formulation Lumigan and test formulation (FX) (b) Wetted length measurement during dry eye test for normal, disease, MKT and test formulation (FX) group (c) Conjunctival hyperemia comparison between disease control group and anti-glaucoma therapy groups (MKT and FX)

Fig 14: Microscopic examination of animal's groups under study with different treatments with respect to time (days)

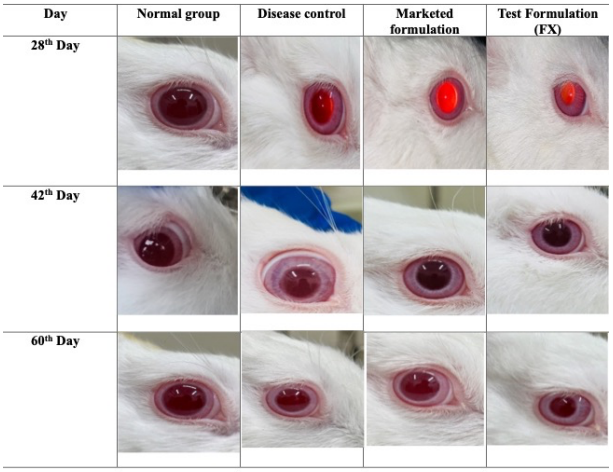

Conclusion

In the current research, researchers formulated and assessed an ion-triggered in situ gel incorporating bimatoprost. The refined nanoemulsion formulation met the specified targets for particle size, polydispersity index (PDI), and zeta potential. Contact with tear fluid prompted on-site gel formation, yielding a nanoemulsion gel (NEG). Over a three-month stability evaluation, the system maintained uniform transparency, reliable gelling performance, stable drug levels, consistent particle dimensions, and steady zeta potential. In vitro drug release experiments revealed prolonged therapeutic release, while assessments for microbial sterility and

osmotic compatibility affirmed its safety for ocular administration. Overall, this system emerges as a viable option over standard eye drop solutions, enhancing drug retention at the corneal surface and supporting extended-release kinetics. Additionally, pharmacodynamic data demonstrated that the FX variant—supplemented with omega-3 fatty acids and hyaluronic acid (HA)—outperformed the commercial benchmark in mitigating treatment-related ocular dryness and conjunctival redness.

Consent for publication: All authors provide the consent for publication

Availability of data and materials: NA

Competing interests: Nil

Clinical trial number: Not applicable

Funding: The authors gratefully acknowledge GD Goenka University, Gurugram, for providing funding support through seed grant policy 3.0 (R&D10/24/03) to this research.

List of abbreviations

NEG - Nanoemulgel
HA - Hyaluronic Acid
IOP - Intraocular Pressure
PDI - Polydispersity Index
GG - Gellan Gum
Smix - Surfactant mixture
RPHPLC - Reverse-Phase High-Performance Liquid Chromatography
DLS - Dynamic Light Scattering
TEM - Transmission Electron Microscopy
PTA - Phosphotungstic Acid
CPCSEA - Committee for the Purpose of Control and Supervision of Experiments on Animals
IAEC - Institutional Animal Ethics Committee
DEX - Dexamethasone
MKT - Marketed Formulation (Lumigan®)
FX - Test Formulation
RBCs - Red Blood Cells
ANOVA - Analysis of Variance
ICH - International Council for Harmonisation of Technical Requirements for Pharmaceuticals for Human Use

References

1. Dietze, J., Blair, K., Zeppieri, M., et al. (2024, March 16). Glaucoma. In *StatPearls [Internet]*. Treasure Island (FL): StatPearls Publishing. https://www.ncbi.nlm.nih.gov/books/NBK538217/
2. GBD 2015 Disease and Injury Incidence and Prevalence Collaborators (2016). Global, regional, and national incidence, prevalence, and years lived with disability for 310 diseases and injuries, 1990-2015: a systematic analysis for the Global Burden of Disease Study 2015. *Lancet (London, England)*, *388*(10053), 1545–1602.
3. Yadav, M., Guzman-Aranguez, A., Perez de Lara, M. J., Singh, M., Singh, J., & Kaur, I. P. (2019). Bimatoprost loaded nanovesicular long-acting sub-conjunctival in situ gelling implant: *In vitro* and *In vivo* evaluation. *Materials Science & Engineering C, 103,* 109730. https://doi.org/10.1016/j.msec.2019.05.015
4. Chang, E., Sarrafpour, S., & Teng, C. C. (2021). Side effects of glaucoma medications. *Glaucoma Today,* Jan–Feb 2021.
5. Cvenkel, B., & Kolko, M. (2020). Current medical therapy and future trends in the management of glaucoma treatment. *Journal of Ophthalmology, 2020,* 6138132. https://doi.org/10.1155/2020/6138132
6. Küçük, E., Zor, K. R., Çoban Karataş, M., & Yıldırım Biçer, G. (2024). Prevalence of dry eye in patients using topical antiglaucoma medications. *Northwestern Medical Journal, 4*(2), 101–105. https://doi.org/10.54307/2024.NWMJ.113
7. Wenqing Zhu, Xiangmei Kong, Jianjiang Xu, Xinghuai Sun, "Effects of Long-Term Antiglaucoma Eye Drops on Conjunctival Structures: An *In vivo* Confocal Microscopy Study", *Journal of Ophthalmology*, vol. 2015, Article ID 165475, 7 pages, 2015. https://doi.org/10.1155/2015/165475
8. Arici, M. K., Arici, D. S., Topalkara, A., & Güler, C. (2000). Adverse effects of topical antiglaucoma drugs on the ocular surface. *Clinical & experimental ophthalmology*, *28*(2), 113–117. https://doi.org/10.1046/j.1442-9071.2000.00237.x

9. M. Vimalin Jeyalatha, Yangluowa Qu, Zhen Liu, Shangkun Ou, Xin He, Jinghua Bu, Sanming Li, Peter Sol Reinach, Zuguo Liu, Wei Li, Function of meibomian gland: Contribution of proteins, Experimental Eye Research, Volume 163, 2017, Pages 29-36, ISSN 0014-4835, https://doi.org/10.1016/j.exer.2017.06.009.
10. Arita R, Itoh K, Maeda S, Maeda K, Furuta A, Tomidokoro A, Aihara M, Amano S. Comparison of the long-term effects of various topical antiglaucoma medications on meibomian glands. Cornea. 2012 Nov;31(11):1229-34. doi: 10.1097/ICO.0b013e31823f8e7d. PMID: 22406943.
11. Wilson RP, Spaeth GL, Poryzees E. The place of timolol in the practice of ophthalmology. Ophthalmology. 1980;87:451–454.
12. Alm A, Stjernschantz J. Effects on intraocular pressure and side effects of 0.005% latanoprost applied once daily, evening or morning. A comparison with timolol. Scandinavian Latanoprost Study Group. Ophthalmology. 1995;102:1743–1752.
13. Sherwood MB, Grierson I, Millar L, et al. Long-term morphologic effects of antiglaucoma drugs on the conjunctiva and Tenon's capsule in glaucoma patients. Ophthalmology. 1989;96:327–335.
14. Brandt JD, Wittpenn JR, Katz LJ, Steinmann WN, Spaeth GL. Conjunctival impression cytology in patients with glaucoma using long-term topical medication. Am J Ophthalmol. 1991 Sep 15;112(3):297-301. doi: 10.1016/s0002-9394(14)76730-3. PMID: 1679298.
15. Wong, A. B. C., Wang, M. T. M., Liu, K., Prime, Z. J., Danesh-Meyer, H. V., & Craig, J. P. (2018). Exploring topical anti-glaucoma medication effects on the ocular surface in the context of the current understanding of dry eye. *The ocular surface*, *16*(3), 289–293. https://doi.org/10.1016/j.jtos.2018.03.002
16. Giannaccare, G., Pellegrini, M., Sebastiani, S., Bernabei, F., Roda, M., Taroni, L., Versura, P., & Campos, E. C. (2019). Efficacy of Omega-3 Fatty Acid Supplementation for Treatment of Dry Eye Disease: A Meta-Analysis of Randomized Clinical Trials. Cornea, 38(5), 565–573. https://doi.org/10.1097/ICO.0000000000001884
17. Downie, L. E., Hom, M. M., Berdy, G. J., El-Harazi, S., Verachtert, A., Tan, J., Liu, H., Carlisle-Wilcox, C., Simmons, P., & Vehige, J. (2020). An artificial tear containing flaxseed oil for treating dry eye disease: A randomized controlled trial. The ocular surface, 18(1), 148–157. https://doi.org/10.1016/j.jtos.2019.11.004
18. Kwon, J. W., & Han, S. B. (2017). Omega-3 fatty acid supplementation can improve both symptoms and signs of dry eye disease. Clinical interventions in aging, 12, 485–486. https://doi.org/10.2147/CIA.S132454
19. Calder P. C. (2010). Omega-3 fatty acids and inflammatory processes. Nutrients, 2(3), 355–374. https://doi.org/10.3390/nu2030355
20. Russo, V., Stella, A., Appezzati, L., Barone, A., Stagni, E., Roszkowska, A., & Delle Noci, N. (2009). Clinical efficacy of a Ginkgo biloba extract in the topical treatment of allergic conjunctivitis. European journal of ophthalmology, 19(3), 331–336. https://doi.org/10.1177/112067210901900301
21. Kim, D.J., Jung, MY., Pak, HJ. et al. Development of a novel HA membrane for the treatment of ocular surface diseases. Sci Rep 11, 2351 (2021). https://doi.org/10.1038/s41598-021-81983-1
22. Huynh, A., & Priefer, R. (2020). HA applications in ophthalmology, rheumatology, and dermatology. Carbohydrate research, 489, 107950. https://doi.org/10.1016/j.carres.2020.107950
23. Yang, Y. J., Lee, W. Y., Kim, Y. J., & Hong, Y. P. (2021). A Meta-Analysis of the Efficacy of HA Eye Drops for the Treatment of Dry Eye Syndrome. International journal of environmental research and public health, 18(5), 2383. https://doi.org/10.3390/ijerph18052383
24. Nguyen, Duc & Luo, Li-Jyuan & Lai, Jui-Yang. (2021). Thermogels containing sulfated hyaluronan as novel topical therapeutics for treatment of ocular surface inflammation. Materials Today Bio. 13. 100183. 10.1016/j.mtbio.2021.100183.

25. Tzong-Yun Ger, Chia-Jung Yang, Sandip Ghosh, Jui-Yang Lai, Biofunctionalization of nanoceria with sperminated hyaluronan enhances drug delivery performance for corneal alkali burn therapy, Chemical Engineering Journal, Volume 476, 2023, 146864, ISSN 1385-8947, https://doi.org/10.1016/j.cej.2023.146864.
26. Nguyen, D. D., Yao, C. H., Luo, L. J., Chen, H. C., Hsueh, Y. J., Ma, D. H., & Lai, J. Y. (2022). Oxidation-mediated scaffold engineering of HA-based microcarriers enhances corneal stromal regeneration. Carbohydrate polymers, 292, 119668. https://doi.org/10.1016/j.carbpol.2022.119668
27. Satyanarayana, S. D., Abu Lila, A. S., Moin, A., Moglad, E. H., Khafagy, E. S., Alotaibi, H. F., Obaidullah, A. J., & Charyulu, R. N. (2023). Ocular Delivery of Bimatoprost-Loaded Solid Lipid Nanoparticles for Effective Management of Glaucoma. *Pharmaceuticals (Basel, Switzerland)*, *16*(7), 1001. https://doi.org/10.3390/ph16071001
28. Sun, J., & Zhou, Z. (2018). A novel ocular delivery of brinzolamide based on gellan gum: *In vitro* and *In vivo* evaluation. *Drug design, development and therapy*, *12*, 383–389. https://doi.org/10.2147/DDDT.S153405 (Retraction published Drug Des Devel Ther. 2022 Dec 02;16:4109-4110. doi: 10.2147/DDDT.S399707)
29. Kumar, S., Natraj, K., Khan, A., Kumar, B., & Rao, J. (2011). Development and validation of RP-HPLC method for estimation of bimatoprost in pharmaceutical dosage forms. *Journal of Pharmaceutical Research Online, 44.*
30. Monika, Sharma, S., Shrivastva, M., Kumar, S., Rabbani, S. A., & Garg, A. (2022). Novel in situ NEG (NEG) of azithromycin with eugenol for the treatment of periodontitis: Formulation development and characterization. *Journal of Cluster Science, 33*(6), 2589–2600. https://doi.org/10.1007/s10876-021-02172-8
31. Srivastava, M., Kohli, K., & Ali, M. (2016). Formulation development of novel in situ NEG (NEG) of ketoprofen for the treatment of periodontitis. *Drug Delivery, 23*(1), 154–166. https://doi.org/10.3109/10717544.2014.907842
32. Thimmasetty, M. K., Mandal, S., Prabhushankar, G. L., & Geetha, M. S. (2012). Formulation and evaluation of an in situ gel-forming ophthalmic formulation of moxifloxacin hydrochloride. *International Journal of Pharmaceutical Investigation, 2*(2), 78–82.
33. Wadetwar, R. N., Agrawal, A. R., & Kanojiya, P. S. (2020). In situ gel containing bimatoprost solid lipid nanoparticles for ocular delivery: In-vitro and ex-vivo evaluation. *Journal of Drug Delivery Science and Technology, 56*(Part A), 101575. https://doi.org/10.1016/j.jddst.2020.101575
34. Garg, M., & Kaur, G. (2014). In situ gelling ophthalmic drug delivery system: Formulation and evaluation. *Journal of Applied Polymer Science, 131,* 39788. https://doi.org/10.1002/app.39788
35. Weinreb RN, Toris CB. Mechanisms of action of prostaglandin analogs in glaucoma. Surv Ophthalmol. 2019;64(6):773–795. doi:10.1016/j.survophthal.2019.02.001
36. Lee AR, Kim JY, Kim MH, Choi JS, Chung SK. Nanotechnology-based drug delivery systems for glaucoma treatment. Prog Retin Eye Res. 2021;82:100922. doi:10.1016/j.preteyeres.2020.100922
37. Aihara M, Lindsey JD, Weinreb RN. Ocular side effects of topical prostaglandin analogs: clinical and histopathologic findings. Jpn J Ophthalmol. 2012;56(1):30–36. doi:10.1007/s10384-011-0109-2
38. Inoue K, Okayama R, Higa R, Tomita G. Ocular surface and tear function changes after long-term use of prostaglandin analogs. Clin Ophthalmol. 2015;9:435–440. doi:10.2147/OPTH.S76663
39. Rashid S, Jin Y, Ecoiffier T, Barabino S, Schaumberg DA, Dana MR. Topical omega-3 and omega-6 fatty acids for treatment of dry eye. Arch Ophthalmol. 2008;126(2):219–225. doi:10.1001/archophthalmol.2007.56
40. Stapleton F, Alves M, Bunya VY, Jalbert I, Lekhanont K, Malet F, Na KS, Schaumberg D, Uchino M, Vehof J, Viso E, Vitale S, Jones L. TFOS DEWS II Epidemiology Report. Ocul Surf. 2017;15(3):334–365. doi:10.1016/j.jtos.2017.05.003

41. Parrish RK, Palmberg P, Sheu WP. A comparison of latanoprost, bimatoprost, and travoprost in patients with elevated intraocular pressure: a 12-week, randomized, masked-evaluator multicenter study. Am J Ophthalmol. 2003;135(5):688–703. doi:10.1016/s0002-9394(02)02275-3
42. McLaren JW, Brubaker RF, FitzSimon JS. Continuous measurement of ocular hyperemia induced by prostaglandin analogs. Invest Ophthalmol Vis Sci. 2016;57(6):2496–2503. doi:10.1167/iovs.15-18906.
43. Singh M, Devi M, Singh RP, Monika, Jhawat V, DoE based development and optimization of ion sensitive in situ nanoemulgel containing bimatoprost for sustained ocular delivery, Int J Bio Macromol, 2025, 329(1), 147768, https://doi.org/10.1016/j.ijbiomac.2025.147768 .